



Numerical Modelling of Flow and Transport on Massively Parallel Computers

Andreas Englert, Horst Hardelauf, Jan Vanderborght,
Harry Vereecken

published in

NIC Symposium 2004, Proceedings,
Dietrich Wolf, Gernot Münster, Manfred Kremer (Editors),
John von Neumann Institute for Computing, Jülich,
NIC Series, Vol. **20**, ISBN 3-00-012372-5, pp. 409-418, 2003.

© 2003 by John von Neumann Institute for Computing

Permission to make digital or hard copies of portions of this work for personal or classroom use is granted provided that the copies are not made or distributed for profit or commercial advantage and that copies bear this notice and the full citation on the first page. To copy otherwise requires prior specific permission by the publisher mentioned above.

<http://www.fz-juelich.de/nic-series/volume20>

Numerical Modelling of Flow and Transport on Massively Parallel Computers

Andreas Englert, Horst Hardelauf, Jan Vanderborght, and Harry Vereecken

Institute Agrosphäre ICG-IV
Research Centre Jülich, 52425 Jülich, Germany
E-mail: {a.englert, h.hardelauf, j.vanderborght, h.vereecken}@fz-juelich.de

1 Introduction and Motivation

Hydrogeologists and soil physicists have developed concepts to describe water flow and transport of dissolved substances in soils and aquifers. Detailed information on fundamental principals and basic equations describing flow and transport are presented, for instance, in Bear, Busch et al.¹, or Delleur⁶. These basic equations are principally based on the concept of a Representative Elementary Volume (REV) in which the flow and transport processes can be described using a spatially homogeneous set of flow and transport parameters. The scale of the volume on which parameters can be experimentally defined is limited by the measurement scale of water and solute fluxes, water contents, pressure heads and solute concentrations. For practical applications, water flow and transport models should describe flow and transport processes at the management scale of soil and groundwater systems. A major problem for the practical application of flow and transport models is therefore the large difference between management and measurement scales. Several studies have revealed that parameters that are determined at the measurement scale vary considerably in space. Therefore, upscaling procedures are required to derive effective parameters that describe the system's behaviour at the management scale. Effective parameters are parameters that lump the system's subscale heterogeneity and describe its behaviour at a larger scale (e.g. Grayson and Blöschel⁸). In the 'scale way' (Vogel and Roth²²) approach, the smaller scale structure and heterogeneity of the properties are explicitly considered to predict processes. The predicted processes and variables at the smaller scale are then averaged and effective parameters are derived that predict the spatially averaged processes/variables at the larger scale.

To investigate the effect of spatial variability of flow and transport parameters on the larger scale processes, a three dimensional description of the processes is required. The 3-D flow and transport equations are presented in section 2. In section 3, the TRACE/PARTRACE computer codes that solve the flow and transport equations numerically are briefly presented. To solve flow and transport processes in three dimensions, large computational grids are required. Therefore, the TRACE/PARTRACE codes were designed for parallel computation, which is shown in section 4. Applications of the TRACE/PARTRACE models are shown in section 5. In subsection 5.1, an example of upscaling transport from the microscopic to the core scale is presented. Section 5.2 discusses upscaling from the core scale to the field scale. The variability of the core-scale parameters is treated in a stochastic framework and solutions of the stochastic flow and transport are used to determine effective field-scale parameters. The field-scale parameters

are subsequently used in a regional scale flow and transport model, of which an example is given in Section 5.3.

2 Flow and Transport Equations

The basic equation to describe the water movement in the subsurface is the Richards equation:

$$\frac{\partial \theta}{\partial t} = \nabla \cdot \mathbf{K} \nabla (\psi + z) - S(\mathbf{x}), \quad (1)$$

where $\theta(L^3L^{-3})$ is the volumetric water content, $\mathbf{K}(LT^{-1})$ the hydraulic conductivity tensor, $\psi(L)$ the pressure head, $z(L)$ the elevation head, and $S(\mathbf{x}) (T^{-1})$ a sink term that accounts for water uptake, among others water uptake by plant roots. In the unsaturated zone, ψ is negative due to capillary forces and is also called the matric head. In the saturated zone, ψ is positive and equal to the hydrostatic pressure head. Under unsaturated conditions, the water content θ and the hydraulic conductivity \mathbf{K} are related to the matric head. The functions $\theta(\psi)$ and $\mathbf{K}(\psi)$ are constitutive relationships that characterise the hydraulic soil properties. These functions are highly non-linear and an approximate solution of Eq. (1) can only be obtained using numerical methods.

Transport through porous media is described by the convection dispersion equation:

$$\theta \frac{\partial C}{\partial t} + \rho \frac{\partial s}{\partial t} = \nabla \theta \mathbf{D} \nabla C - \mathbf{q} \nabla C + Q^*, \quad (2)$$

where $C(ML^{-3})$ is the concentration, $s(MM^{-1})$ sorbed concentration (mass of sorbed compound per mass of sediment/soil), $\rho(ML^{-3})$ the bulk density, $\mathbf{D}(L^2T^{-1})$ the dispersion tensor, $\mathbf{q}(LT^{-1})$ the water flux vector, and $Q^*(ML^{-3}T^{-1})$ a source/sink term. The dispersion includes all diffusive and dispersive processes happening on the scales smaller than the averaging scale of the water flow. In practice, the lower limit of this averaging scale corresponds with the spatial discretization that is used to solve the flow equation numerically. An additional equation is required relating the sorbed concentration to the concentration in solution. When sorption and desorption are instantaneous, s and C can be directly related through the sorption isotherm. For the case of rate limited sorption/desorption, an additional equation describing the sorption kinetics is included.

3 Numerical Solutions

The TRACE code (Vereecken et al.²¹) was developed to solve the 3-D Richards equation numerically. The TRACE computer code uses the three dimensional Finite Element (FE) Galerkin method with hexagonal isoparametric elements and a finite difference time discretization. Due to the non-linearity of the Richards equation (Eq. 1) a modified Picard-iteration scheme (Celia et al.⁴) is used to linearize the equations and update the solution iteratively until convergence is reached. The resulting system of linear equations is preconditioned based on diagonal scaling of the matrix. To solve this system of linear equations the Conjugated Gradient (CG) method is used. Time discretization is variable to include changes in boundary conditions and to consider convergence behaviour of the iterative solution.

The PARTRACE computer code (Neuendorf¹⁵) is a 3D particle tracking code using the velocity field from TRACE. For this purpose the underlying convection dispersion equation (Eq. 2) is identified as the Ito Fokker Planck equation. A reformulation of the Ito Fokker Planck equation leads to the nonlinear Langevin equation. The Langevin equation in combination with the Ito Fokker Planck equation, reformulated for a single particle, gives the motion equation used in the particle tracking method (van Kampen¹¹). Thereby the convective movement of a particle is computed using the flow velocity field from TRACE, whereas the microdispersion is calculated using random particle motion. Also the simulation of sorption processes is implemented in the particle tracking code using junction probabilities within the suitable sorption mechanism.

4 Parallel Processing

The computer code TRACE enables execution on massive parallel computers (Seidemann¹⁷). To facilitate the partitioning of the FE-grid into sub-grids of approximately the same size the following restriction for the discretization of the FE-grid is introduced: the hexagonal elements have to fill the FE-grid without any gap and, consequently, the number of nodes is equal for each direction in space respectively. Between the sub-grids an overlap of one element permits the computation of outer nodes of one sub-grid by computing inner nodes inside the adjacent sub-grid and vice versa. Each processor sets up a system of linear equations for one sub-grid.

Parallelization of the PARTRACE computer code follows principally the strategy to distribute equally the number of particles on the processors. For relatively small numbers of nodes in the flow velocity field all data of the flow velocity field are stored on each processor. This is very fast for the computation, but is not possible for a great many of nodes, due to the finite storage space of the working memories. In this case it is possible to distribute the flow velocity field to several processors. The interchange of data between the processors is done using MPI.

5 Application of the TRACE/PARTRACE Models

5.1 Upscaling Transport Processes from the Microscopic to the Core Scale

Three-dimensional solute transport in a column packed with glass beads was simulated by Herrmann et al.⁹ using the TRACE/PARTRACE models. They obtained the microscopic 3-D structure of the hydraulic conductivity inside the column using the Nuclear Magnetic Resonance Imaging (NMRI) (Figure 1). From simulated concentration distributions in the column (Figure 1), an effective dispersion coefficient was derived. This coefficient was considerably larger than the diffusion coefficient but comparable with the effective dispersion coefficient that was derived from breakthrough experiment in the column. This study illustrates and provides experimental evidence that larger scale transport processes may be predicted based on the spatial structure of smaller scale transport properties.

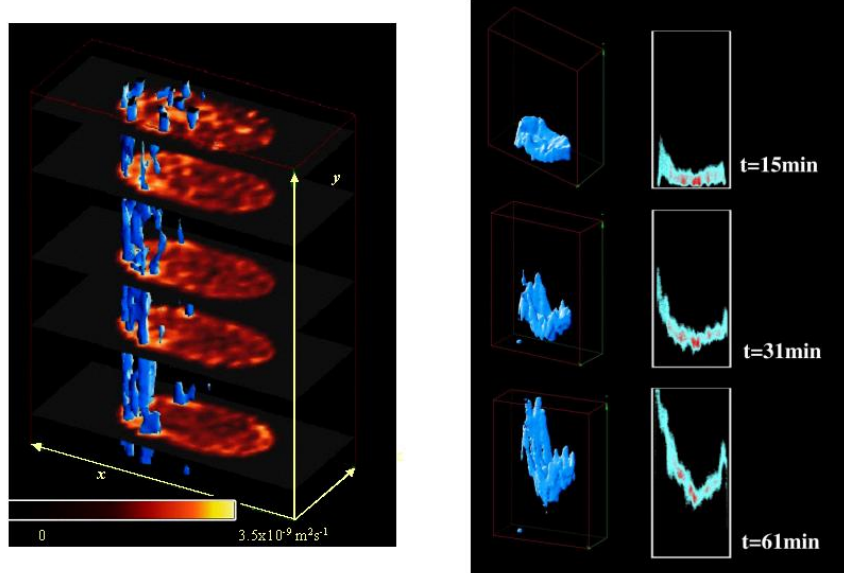


Figure 1. **Left Panel:** velocity field in a column packed with glass beads derived from NMRI (blue iso-surfaces include regions with high flow velocity). **Right Panel:** Simulated tracer concentrations with the TRACE/PARTRACE models.

5.2 Upscaling Flow and Transport from the Core Scale to the Field Scale: Tests of Approximate Analytical Solutions of Stochastic Flow and Transport Equations

Due to heterogeneity of the subsurface and practical limitations to determine the parameters at each location, the spatial behavior of the parameters of the Richards and CDE equations is treated in a probabilistic or stochastic framework. A spatial parameter distribution $u(\mathbf{x})$ is considered to be realization of a Random Space Functions (RSF), $U(\mathbf{x})$, which characterizes the stochastic or random spatial behavior of $u(\mathbf{x})$. In general, a RSF is defined through a set of multidimensional probability distributions, F , which give the probability of a set of observations at a set of points:

$$\begin{aligned}
 P(U(\mathbf{x}) < u) &= F_{\mathbf{x}}(u) \\
 P(U(\mathbf{x}_1) < u_1, U(\mathbf{x}_2) < u_2) &= F_{\mathbf{x}_1 \mathbf{x}_2}(u_1, u_2) \\
 P(U(\mathbf{x}_1) < u_1, \dots, U(\mathbf{x}_i) < u_i, \dots, U(\mathbf{x}_n) < u_n) &= F_{\mathbf{x}_1, \dots, \mathbf{x}_i, \dots, \mathbf{x}_n}(u_1, \dots, u_i, \dots, u_n),
 \end{aligned} \tag{3}$$

where $P(U(\mathbf{x}_1) < u_1, \dots, U(\mathbf{x}_i) < u_i, \dots, U(\mathbf{x}_n) < u_n)$ is the probability of a simultaneous outcome of $U(\mathbf{x}_1) < u_1, \dots, U(\mathbf{x}_i) < u_i, \dots, U(\mathbf{x}_n) < u_n$.

In practice, the multidimensional probability density functions are assumed to be multivariate Gaussian and translation invariant. This implies that the RSF is so-called stationary and fully characterized by a constant mean and a spatial covariance which depends only on the separation between the observations. When the hydraulic conductivity is a RSF, the Richards equation is a stochastic partial differential equation. The solution of the stochastic Richards equation renders the statistical characteristics of the RSFs of the output

variables: pressure head ψ , and water flux \mathbf{q} . More specifically, the spatial covariance C_{uu} and cross-covariances C_{uv} of the output and input parameters are determined:

$$C_{uu}(\mathbf{x}, \mathbf{x} + \mathbf{h}) = \langle (u(\mathbf{x}) - \langle u(\mathbf{x}) \rangle) (u(\mathbf{x} + \mathbf{h}) - \langle u(\mathbf{x} + \mathbf{h}) \rangle) \rangle \quad (4)$$

$$C_{uv}(\mathbf{x}, \mathbf{x} + \mathbf{h}) = \langle (u(\mathbf{x}) - \langle u(\mathbf{x}) \rangle) (v(\mathbf{x} + \mathbf{h}) - \langle v(\mathbf{x} + \mathbf{h}) \rangle) \rangle \quad (5)$$

where $\langle \cdot \rangle$ is the expected value for all realizations of the input parameter field.

In the transport equation, the water flux \mathbf{q} is a stochastic input parameter and its spatial statistics are obtained by solving the stochastic Richards equation. Also sorption and decay parameters may be treated as stochastic input parameters whereas the pore-scale dispersion coefficient and the water content are mostly considered deterministic.

The output of the stochastic transport equation are the expected concentrations $\langle C(\mathbf{x}, t) \rangle$, the spatial/temporal centralized second moments of expected concentrations $\overline{X}_{ij}(t)$, $\overline{T^2}(\mathbf{x})$ and the expected spatial/temporal centralized second moments of the concentration fields/ breakthrough curves $\langle X_{ij}(t) \rangle$, $\langle T^2(\mathbf{x}) \rangle$ that result from a point source injection:

$$\overline{X}_{ij}(t) = \int x_i x_j \langle c_x(x, t) \rangle d\mathbf{x} - \int x_i \langle c_x(\mathbf{x}, t) \rangle d\mathbf{x} \int x_j \langle c_x(\mathbf{x}, t) \rangle d\mathbf{x} \quad (6)$$

$$\overline{T^2}(\mathbf{x}) = \int t^2 \langle c_t(\mathbf{x}, t) \rangle dt - \left(\int t \langle c_t(\mathbf{x}, t) \rangle dt \right)^2 \quad (7)$$

$$\langle X_{ij}(t) \rangle = \left\langle \int x_i x_j c_x(\mathbf{x}, t) d\mathbf{x} - \int x_i c_x(\mathbf{x}, t) d\mathbf{x} \int x_j c_x(\mathbf{x}, t) d\mathbf{x} \right\rangle \quad (8)$$

$$\langle T^2(\mathbf{x}) \rangle = \left\langle \int t^2 c_t(\mathbf{x}, t) dt - \left(\int t c_t(\mathbf{x}, t) dt \right)^2 \right\rangle, \quad (9)$$

where

$$c_x(\mathbf{x}, t) = \frac{C(\mathbf{x}, t)}{\int C(\mathbf{x}, t) d\mathbf{x}}$$

and

$$c_t(\mathbf{x}, t) = \frac{C(\mathbf{x}, t)}{\int C(\mathbf{x}, t) dt}$$

These moments are a measure of the spreading of a solute plume due to heterogeneity in flow velocity. In the first set of moments $\overline{X}_{ij}(t)$, $\overline{T^2}(\mathbf{x})$ the uncertainty of the location of the center of mass of the plume or the uncertainty of the peak concentration time are included in the measure of spreading. Therefore, they represent the spreading of plumes or breakthrough curves that result from an area wide injection, which can be considered as a large number of point source injections. The second set of moments $\langle X_{ij}(t) \rangle$, $\langle T^2(\mathbf{x}) \rangle$ characterize the average spreading of a plume/breakthrough curve resulting from a point source injection around its center of mass or peak arrival time. It represents the mixing or dilution of mass that is injected in a heterogeneous aquifer.

The moments form the basis for upscaling of the transport equation. In the upscaled transport equation, the flow velocity \mathbf{q} is assumed to be deterministic at the larger scale. The effect on the transport process of smaller scale velocity variations due to small scale hydraulic conductivity variations is lumped in an effective dispersion parameter, \mathbf{D}_{eff} . \mathbf{D}_{eff}

is defined so that moments of concentration distributions/breakthrough curves that are predicted by the upscaled transport equation correspond with those in the heterogeneous medium. Two different effective dispersion coefficients can be defined (e.g. Vanderborght and Vereecken¹⁹):

$$\mathbf{D}_{\text{eff1}} = \frac{\overline{X_{ij}(t)}}{2t} \quad (10)$$

$$\mathbf{D}_{\text{eff2}} = \frac{\langle X_{ij}(t) \rangle}{2t} \quad (11)$$

where \mathbf{D}_{eff1} is an effective dispersion coefficient which describes the spreading of an area-wide injected solute plume and \mathbf{D}_{eff2} a coefficient which describes the dilution of injected mass.

Approximate analytical solutions of the stochastic flow and transport equations are obtained by expanding the solution of the partial differential equation in an asymptotic series of the input parameter perturbations. When the perturbations are small, the asymptotic series may be truncated and higher order perturbation terms neglected. Then closed form approximate analytical solutions of a given order can be obtained (e.g. Dagan⁵).

Another way to obtain solutions of stochastic flow and transport equations is to apply brute numerical force and carry out Monte-Carlo simulations in a set of realizations of the parameter fields. In one realization of the parameter field, the flow and transport equations are solved numerically. The spatial statistics of the dependent variables can then be derived from the simulated variable fields. The TRACE/PARTRACE codes have been applied for carrying out such Monte Carlo simulations. Because of the numerical burden, these simulations are mostly done in 2-D and relatively small conductivity fields (e.g. Bellin et al.²). Using the parallelized TRACE/PARTRACE codes, flow and transport could be simulated in 3-D fields of large spatial extent. In order to generate realizations of the parameter fields, a Kraichnan random field generator (Kraichnan¹³, Schwarze¹⁶) was coupled to the TRACE/PARTRACE codes. The advantage of the Kraichnan generator is that large random fields can be generated with sufficient spectral resolution based on a much smaller set of random numbers than the number of grid nodes. As a consequence, the Kraichnan generator requires less storage of random numbers and less arithmetic operations to calculate the parameter values at the grid nodes than regular grid based spectral random fields generators in which a random number must be drawn and stored for each grid node.

Englert⁷ carried out Monte Carlo simulations in 3-D hydraulic conductivity fields with geostatistical parameters that were derived from hydraulic conductivity estimates at the test-site Krauthausen. In contrast to simulations in 2-D and 3-D isotropic hydraulic conductivity fields (e.g. Naff et al.¹⁴), he found that in an hydraulic conductivity field with an anisotropic spatial correlation (larger correlation in the horizontal than in the vertical direction) the variance of the Darcy flow velocity \mathbf{h} is significantly larger than its first-order approximate prediction. This is, however, in agreement with second-order correction terms (Hsu and Neuman¹⁰) that increase with increasing anisotropy. The Monte-Carlo simulations carried out by Englert⁷ were the first to confirm this analytical result.

Transport simulations in a generated heterogeneous aquifer (Figure 2) were carried out by Vanderborght et al.²⁰ using the TRACE/PARTRACE models.

Effective dispersivities, $\lambda_{\text{eff1}} = \mathbf{D}_{\text{eff1}}/v$ and $\lambda_{\text{eff2}} = \mathbf{D}_{\text{eff2}}/v$ (v is the mean pore water velocity), were derived from breakthrough curves at reference planes perpendicular

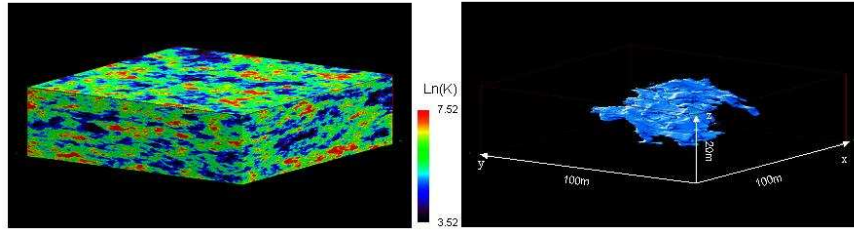


Figure 2. **Left panel:** Generated heterogeneous hydraulic conductivity field. **Right panel:** simulated tracer plume.

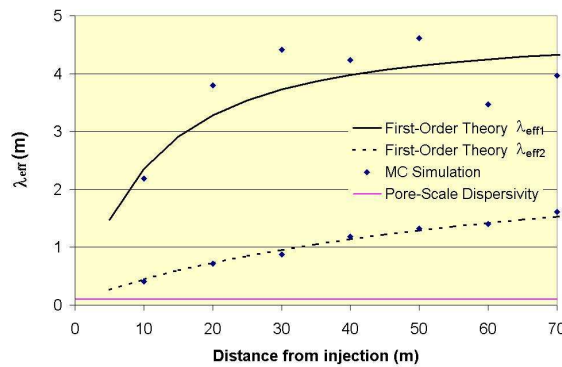


Figure 3. Effective dispersivities, λ_{eff} , derive from first-order approximate solutions of the stochastic flow and transport equations (black lines) and from Monte Carlo simulations (symbols).

to the mean flow direction. The effective parameters derived from numerical simulation were similar to those derived from a first-order approximate solution of the stochastic flow and transport equations (Figure 3). As a consequence this study suggests that first-order approximations may be used to infer geostatistical parameters, which characterize the heterogeneity of an aquifer, inversely from effective transport parameters that are obtained from groundwater tracer experiments.

5.3 Modelling Flow and Transport at the Regional Scale

Small-scale stochastic variations of flow and transport parameters cannot be considered explicitly at the regional scale but must be implicitly incorporated in the model using effective flow and transport parameters. As illustrated above, these effective parameters can be defined by solving stochastic flow and transport equations. At the larger scale, variability in flow and transport parameters is due to variations in soil types and geology. Using soil maps and geological information, this variability may be treated in a deterministic sense. Also spatial variations in land-use and vegetation are important factors that influence flow and transport. Since surface boundary conditions and internal sinks (root water uptake) in a water flow model are to a major extent controlled by plants, a water flow model should be coupled to a crop growth model. Therefore, a simple crop growth model SUCROS

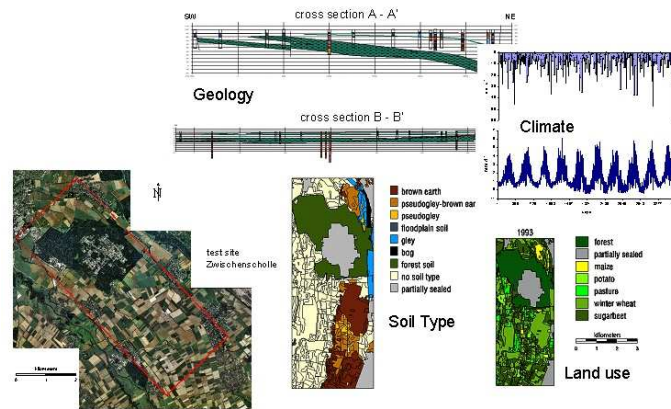


Figure 4. Information sources for a 3-D hydro-geological model.

(Spitters et al.¹⁸), which calculates dry matter accumulation of a crop as a function of irradiation, temperature and crop characteristics, was coupled to the soil/groundwater flow model TRACE.

A basic issue in modelling flow and transport at a larger scale, is the coupling between predominantly vertical flow and transport processes in the vadoze zone and the horizontal processes in the groundwater. A fully 3-D variably saturated flow model like TRACE circumvents an iterative coupling between vadoze zone and groundwater simulation models.

In the frame of the PEGASE project, subsurface water fluxes and pesticide transport are modelled in a 20 km² area around the research centre Jülich in order to predict the groundwater quality. In a first step, a 3-D hydro-geological model is built using the soil map geological data and land-use information (Figure 4). From the soil map, four characteristic soil profiles with typical soil layers were identified. Using a pedotransfer function, the hydraulic functions were determined for the different soil layers. Geological information was used to determine the basis of the unconfined aquifer. The soil surface boundary conditions: precipitation and potential evapotranspiration are derived from meteorological data.

The matrix potential at the soil surface, the actual evaporation and transpiration predicted by the TRACE model are shown in Figure 5 for two exemplary days. Since the model considers three dimensional flow, spatially variable soil properties and land use, the spatial structure and heterogeneity of the flow processes at the soil atmosphere-surface are represented by the model. Furthermore, the model also represents the dynamics of water flow in the soil in response to the dynamics of the boundary conditions.

6 Concluding Remarks

The TRACE/PARTRACE codes were used to investigate the effect of the spatial variability of input parameters on flow and transport processes in soils and aquifers at different scales. Parameter distributions were either generated or derived from soil maps and geological data. However, these information sources only contain indirect information about

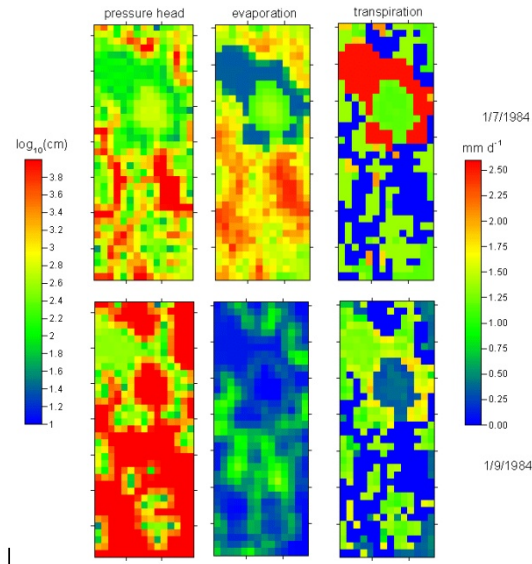


Figure 5. Soil surface matrix potential, evaporation, and crop transpiration at two exemplary days simulated by the TRACE/SUCROS model.

the input parameters of the flow and transport models which brings along uncertainty in the estimated parameter distribution. Alternatively, parameters may be estimated using inverse modelling, i.e. by fitting model predictions to observed variables. Using geophysical methods, processes in the subsurface can be non-invasively and tomographically monitored (e.g. Kemna et al.¹²). Using remote sensing techniques, surface state variables and fluxes and their spatial variation can be obtained. The further development of the TRACE/PARTRACE codes will include the development of inverse modelling procedures to derive spatially distributed parameters fields from the spatio-temporal process information obtained with remote sensing and geophysical methods.

References

1. J. Bear, *Dynamics of fluids in porous media*, American Elsevier Publishing Company, inc. (1972).
2. Bellin, P. Salandin, and A. Rinaldo, *Simulation of dispersion in heterogeneous porous formations: Statistics, first-order theories, convergence of computations*, Water Resour. Res. **28**, 2211-2227 (1992).
3. K.-F. Busch, L. Luckner and K. Tiemer, *Geohydraulik*, Gebrüder Bornträger, Lehrbuch der Hydrogeologie, Volume 3, G. Matthes (1993).
4. M. A. Celia, E. T. Bouloutas and R. L. Zarba, *A general mass-conservative numerical solution for the unsaturated flow equation*, Water Resour. Res. **26**, 1483-1496 (1990).
5. G. Dagan, *Flow and transport in porous formations*, Springer Verlag, Heidelberg (1989).

6. J. W. Delleur, *The Handbook of Groundwater Engineering*, CRC Press and Springer, Boca Raton and Heidelberg (1999).
7. A. Englert, *Measurement, estimation and modelling of groundwater flow velocity at Krauthausen test site*, Ph.D. Thesis RWTH Aachen (2003).
8. R. Grayson, and G. Blöschel, *Spatial patterns in catchment hydrology: Observations and modelling*, Cambridge University Press, U.K (2000).
9. K.-H. Herrmann, A. Pohlmeier, D. Gembris, and H. Vereecken, *Three-dimensional imaging of pore water diffusion and motion in porous media by nuclear magnetic resonance imaging*, J. Hydrol. **267**, 244-257 (2002).
10. K.C. Hsu and S.P. Neuman, *Second-order expressions for velocity moments in two- and three-dimensional statistically anisotropic media*, Water Resour. Res. **33**, 625-637 (1997).
11. N. G. van Kampen, *Stochastic processes in physics and chemistry*, North-Holland Publishing Company, Amsterdam (1981).
12. A. Kemna, J. Vanderborght, B. Kulesa, and H. Vereecken, *Imaging and characterisation of subsurface solute transport using electrical resistivity tomography (ERT) and equivalent transport models*, J. Hydrol. **267**, 125-146 (2002).
13. R.H. Kraichnan, *Diffusion by a random velocity field*, The Physics of Fluids **13**, 22-31 (1970).
14. R.L. Naff, D.F. Haley, and E.A. Sudicky, *High-resolution Monte Carlo simulation of flow and conservative transport in heterogeneous porous media: 1. Methodology and flow results*, Water Resour. Res. **34**, 663-677 (1998).
15. O. Neuendorf, *Numerische 3-D Simulation des Stofftransportes in einem heterogenen Aquifer*, Ph.D. thesis, RWTH Aachen (1996).
16. H. Schwarze, U. Jaekel and H. Vereecken, *Estimation of Macrodispersion by Different Approximation Methods for Flow and Transport in Randomly Heterogeneous Media*, Transport in Porous Media **43**, 265-287 (2001).
17. R. Seidemann, *Parallelisierung eines finite Elemente Programms zur Modellierung des Transports von Stoffen durch heterogene poröse Medien*, Ph.D. thesis, Rheinische Friedrich-Wilhelms Universität Bonn (1996).
18. C.J.T. Spitters, H. van Keulen and H. van Kraalingen, *A simple but universal crop growth simulation model, SUCROS87*, In R. Rabbinge, H. Van Laar & Ward (ed), Simulation and system management in crop protection. Simulation Monographs. PU-DOC, Wageningen (1988).
19. J. Vanderborght and H. Vereecken, *Estimation of local scale dispersion from local breakthrough curves during a tracer test in a heterogeneous aquifer: the Lagrangian approach*, J. Contam. Hydrol. **54**, 141-171 (2002).
20. J. Vanderborght, A. Kemna, H. Hardelauf and H. Vereecken, *Using electrical resistivity tomography (ERT) for characterizing transport processes in heterogeneous aquifers*, EGS-AGU-EUG Joint Assembly, Nice, France, 7-11 April 2003. Geophysical Research Abstracts, Vol. 5, 04907 (2003).
21. H. Vereecken, G. Lindenmayr, O. Neuendorf, U. Döring and R. Seidemann, *TRACE a mathematical model for reactive transport in 3D variably saturated porous media*, Internal Report KFA-ICG-4-501494, Jülich (1994).
22. H.J. Vogel and K. Roth, *Moving through scales of flow and transport in soil*, J. Hydrol. **272**, 95-106 (2003).